Letter

Nanophotonic platforms for enhanced chiral sensing

Ershad Mohammadi, Kosmas L.Tsakmakidis, AmirNader Askarpour, Parisa Dehkhoda, Ahad Tavakoli, and Hatice Altug

ACS Photonics, **Just Accepted Manuscript** • DOI: 10.1021/acsphotonics.8b00270 • Publication Date (Web): 22 May 2018

Nanophotonic platforms for enhanced chiral sensing

E. Mohammadi,[1,2] K. L. Tsakmakidis,[1] A. N. Askarpour,[2] P. Dehkhoda,[2] A. Tavakoli,[2] H. Altug[1*]

[1]*Bioengineering Department, École Polytechnique Fédérale de Lausanne (EPFL), 1015 Lausanne, Switzerland*

[2]*Department of Electrical Engineering, Amirkabir University of Technology, Tehran, Iran*

[*]Corresponding author: Email: hatice.altug@epfl.ch

KEYWORDS: chirality, chiral sensing, circular dichroism, nanophotonics

Abstract

Chirality plays an essential role in life, providing unique functionalities to a wide range of biomolecules, chemicals and drugs, which makes chiral sensing and analysis critically important. The wider application of chiral sensing continues to be constrained by the involved chiral signals being inherently weak. To remedy this, plasmonic and dielectric nanostructures have recently been shown to offer a viable route for enhancing weak circular dichroism (CD) effects, but most relevant studies have thus far been ad hoc, not guided by a rigorous analytical methodology. Here, we report the first analytical treatment of CD enhancement and extraction from a chiral bio-layer placed on top of a nano-structured substrate. We derive closed-form expressions of the CD and its functional dependence on the background-chiroptical response, substrate thickness and chirality, as well as on the optical chirality and intensity enhancement provided by the structure. Our results provide key insights into the tradeoffs that are to be accommodated in the design and conception of optimal nanophotonic structures for enhancing CD effects for chiral molecule detection. Based on our analysis, we also introduce a new, simple platform for chiral sensing featuring large CD enhancements while exhibiting vanishing chiroptical background noise.

Introduction

Chirality is a ubiquitous phenomenon in nature, and plays an essential role in life.[1] Today, we know that biological functionality of chiral biomolecules (e.g., proteins, amino acids and carbohydrates), as well as synthesized chiral molecules in drugs, is strongly influenced by their chirality.[2,3]As a result, discrimination of enantiomers is indeed critically important in biology and the pharmaceutical industry in terms of safety and production costs.[4,5] Enantiomers are distinguishable in the way they interact with chiral fields. Traditionally, circular dichroism (CD) spectroscopy has been used for this discrimination, which is essentially the differential absorption for circularly polarized light

(CPL).[6,7] However, the main challenge of CD spectroscopy still remains the *weak* chiroptical signals, due to the weak chirality of matter[8] interacting with plane wave lightfields.

With the advent of plasmonics and metamaterials,[9,10] finding new ways and structures to enhance these weak chirality effects has been an area of extensive research.[11-14] A wide range of structures, including three-dimensional nanohelix arrays,[15-17] twisted crosses[18] and twisted nanorods,[19] chiral oligomers[20] and chiral assemblies of nanoparticles,[21,22] single[23] or multilayer gammadion arrays,[24] and even more complicated structures, such as intertwined 3D helices,[25] have been investigated for enhancing chiroptical effects. Such nanophotonic structures can be realized by bulk metamaterials[15-17] or thin planar metasurfaces,[23] chiral[15-25] or achiral[26,27] inclusions, and plasmonic[15-25] or dielectric[28] media. When a chiral sample is placed in the near-field of such nanostructures, the CD signal can be enhanced according to the enhancement in the field intensity and optical chirality[29,30] provided by the nanophotonic platform.[31,32] Among these two enhancement features, the formation of highly chiral near-fields close to the nanophotonic structure, plays an essential role in enhancing the CD signal. However, it is important to note that all of these platforms have their own intrinsic chiroptical response, which appears as an additive term in the final CD signal and acts as a background noise for the chiral response of bio-layers.

So far, the extensive studies of chiral nanophotonic platforms have been mainly pursued numerically or experimentally, ascertaining the performance of the final device from the *intrinsic* (without the bio-layer) chiroptical response of the substrate (such as, its *intrinsic* CD and provided optical chirality).[33] Yet, the connection of these inherent characteristics of chiral substrate to the *CD signal in the presence of a bio-layer* (necessary for chiral sensing) still remains elusive. Furthermore, several simplified systems have been studied analytically.[22,34] It is the objective of this paper to report the first analytic study of the problem of substrate CD spectroscopy for an arbitrary nanophotonic substrate (either, chiral or achiral, plasmonic or dielectric) and clarify the interplay between key affecting parameters, such as the thickness and chirality of the substrate, as well as the near-field optical chirality enhancement. We formulate a simple analytical description of the phenomenon elucidating the involved tradeoffs, such as between the choice of bulk metamaterials or thin planar metasurfaces, chiral or achiral structures, and between choosing plasmonic or dielectric media.

The paper is organized as follows: In section I, we first analyze an isolated, single chiral bio-layer. Then, we proceed by retrieving the CD signal from the same bio-layer placed on top of a simple chiral substrate that does not enhance the field intensity or chirality in its near-field zone. On the basis of derived analytical expressions, we report a newly identified consequence of substrate chiral absorption (besides background CD noise), which appears in the form of an attenuation factor acting on the CD signal of the bio-layer. In Section II, we generalize the analytical results to nanophotonic substrates by introducing intensity and optical chirality enhancement factors. Based on our analytical results, we propose practical ways to remove the background chiroptical noise of the substrate, as well as eliminating the dependency of the output CD on the permittivity of the bio-layer. Finally, we introduce a practical dielectric platform for chiral sensing offering unique advantages including an enhanced CD signal which is only associated with the molecular handedness, while featuring vanishing chiroptical background response. We will show that the CD enhancement originates from highly chiral near-fields provided by the electric and magnetic dipolar resonances of the dielectric structures.

I. CD signal of a bio-layer placed on top of a simple chiral substrate

In substrate CD spectroscopy, the bio-layer is placed on top of a substrate, and the whole system is illuminated by right-circularly-polarized (RCP) and left-circularly-polarized (LCP) light sequentially. The CD signal is defined as the differential absorption (transmission) of the light for these two polarization states. If I_R and I_L are the transmitted power intensities for RCP and LCP excitations at the output side of the bio-layer, respectively, then the *CD* signal is defined as [32]

$$CD = \tan^{-1}\left(\frac{I_R - I_L}{I_R + I_L}\right) . \qquad (1)$$

First, we consider a conventional CD spectroscopy case, where the CD signal is retrieved from a chiral bio-layer without any substrate. The chiral sample is modelled as a homogenous slab of thickness w_i, placed in free space (inset of Figure 1b) and described by the constitutive equations

$$\begin{aligned} \boldsymbol{D} &= \varepsilon_i \boldsymbol{E} - j\kappa_i \sqrt{\varepsilon_0 \mu_0}\ \boldsymbol{H} \\ \boldsymbol{B} &= \mu_i \boldsymbol{H} + j\kappa_i \sqrt{\varepsilon_0 \mu_0}\ \boldsymbol{E} \end{aligned} \qquad (2)$$

where, ε_i and μ_i are the permittivity and permeability of the chiral sample, respectively, and κ_i is the so-called Pasture parameter,[35] which denotes the material chirality and has different sign for right- and left-handed chiral media. In order to calculate the CD signal analytically, we find the transmission amplitudes for RCP and LCP excitations separately at normal incidence by solving a boundary value problem expressed in an 8x8 matrix. The detailed description can be found in the Supporting Information (SI). By inserting the calculated transmitted intensities in Eq (1), we arrive at the following analytical expression for the CD response of the bio-layer

$$CD_i = -\tan^{-1}\left[\ \tanh\left(\ 2k_0 w_i\ \mathrm{Im}\{\kappa_i\}\ \right)\right] . \qquad (3)$$

Figure 1a shows the transmission spectra of a typical chiral bio-layer as a function of its thickness. The optical parameters of the bio-layer are given in the caption of Fig. 1. To validate the analytical expressions throughout the paper, we performed full-wave simulations with COMSOL Multiphysics which uses finite element method (FEM). It should be noted that the default built-in fully vectorial wave equations in COMSOL should be modified according to the constitutive relations for a chiral media.[36] In Fig. 1b we present the CD_i signal corresponding to the transmission spectra of Fig. 1a. The CD signal increases with the thickness of the biofilm, owing to the respective increase of the effective length of the light-matter interaction. The curve reaches a plateau for larger biofilm thicknesses, because chiral loss[37] attenuates (the transmission of) both CPL polarizations to zero (cf. Fig. 1a). Considering that the chiral layer is normally very thin (i.e., $k_0 w_i \ll 1$), we may approximate Eq. (3), by keeping only the first two leading terms, as

$$CD_i = -\ 2k_0 w_i\ \mathrm{Im}\{\kappa_i\} . \qquad (4)$$

Next, we study the effect of juxtaposing a chiral substrate to the chiral biofilm. As it will become apparent in section II, this intermediate step is useful for analytically identifying the parameters affecting substrate-enhanced CD spectroscopy. Figure 2a shows a chiral sample, now placed on top of a *simple* chiral substrate. To solve this problem analytically, we first assume a simple homogenous chiral matter for the substrate. Here, a "simple" chiral substrate refers to one that does not enhance the intensity or chirality of the light in its near-field zone – as opposed to plasmonic or metamaterial chiral substrates (see next section). In our analysis (cf. Fig. 2b), the configuration of Fig. 2a is modeled as two homogenous juxtaposed chiral slabs of thicknesses w_i (for the bio-layer) and w_s (for the substrate), placed in free space. Compared to the biofilm alone (above), with the substrate we need to solve a 12×12 system of boundary-value equations (see SI). Provided that $k_0\, w_i << 1$, the following compact expression for the output CD signal is obtained

$$CD_i^s = CD_s + CD_i \ \mathrm{sech}\left(4\, k_0\, w_s\, \mathrm{Im}\{\kappa_s\}\right), \qquad (5)$$

where κ_s is the Pasture parameter of the substrate,.

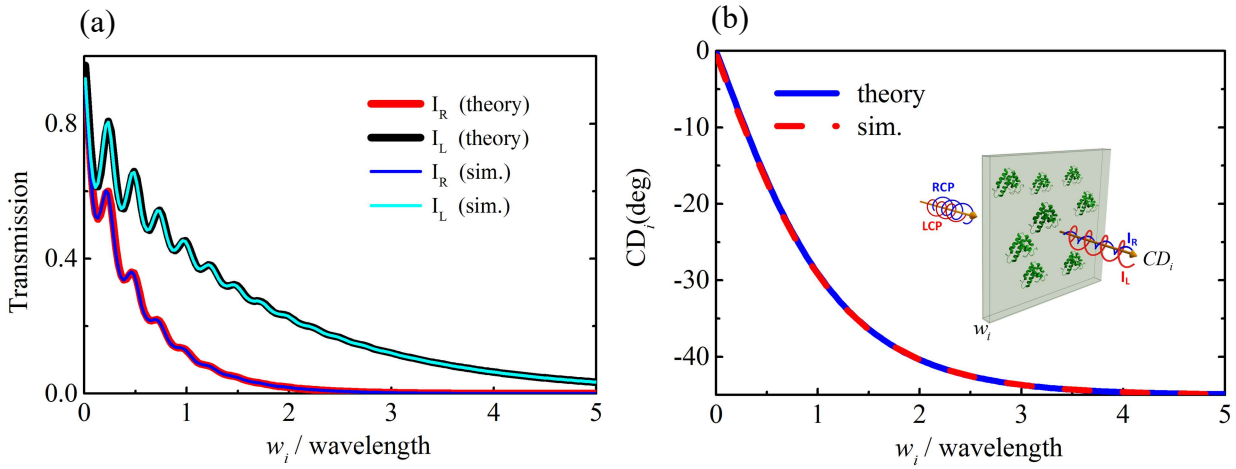

Figure 1. Conventional CD spectroscopy. (a) Transmission intensities of RCP (I_R) and LCP (I_L) waves for a chiral bio-layer of refractive index $n_i = 2 - .1\mathrm{j}$ and Pasture parameter of $\kappa_i = .1 - .05\mathrm{j}$, as a function of the bio-layer's thickness (w_i). (b) CD_i signal corresponding to the transmission spectra in (a), calculated from Eq. (1). The inset shows the chiral sample made of chiral bio-molecules and illuminated by RCP (blue) and LCP (red) lightfields of equal intensities.

Equation (5) provides the total output CD_i^s of the structure in Fig. 2a in terms of individual CD responses of the substrate (CD_s) and the bio-layer (CD_i). Here, CD_i is given by Eq. (3), and CD_s pertains to the differential absorption characterizing the substrate without any bio-layer, which can be obtained by inserting the corresponding parameters of the substrate (κ_s, w_s) into Eq (3). It is, now, evident from Eq. (5) that placing the bio-layer on top of a chiral substrate has two main drawbacks. Firstly, the CD_s signal of the substrate appears as an additive term in the total output of CD_i^s and does not contain any information about the handedness of the bio-layer. Thus, it can be considered as an unwanted signal overwhelming the desired sensed signal (second term in Eq. (5)). The

second drawback can be inferred from the second term of Eq. (5). The multiplication of the CD_i signal with the *sech* term, reveals a hitherto-unidentified consequence of chiral loss in substrate CD spectroscopy: as the *sech* function decreases with increasing argument, the desired sensed signal (CD_i^s - CD_s) decreases with the increasing $k_0\ w_s\ \mathrm{Im}\{\kappa_s\}$ term. More specifically, the *sech* term appears because the RCP and LCP excitations pass through the substrate and arrive in the entrance side of the chiral sample with different attenuation factors exerted on them by the substrate. Thus, increasing the optical thickness ($k_0\ w_s$) or the imaginary part of κ_s, not only increases the background noise (CD_s) but also decreases the desired sensed signal from the bio-layer.

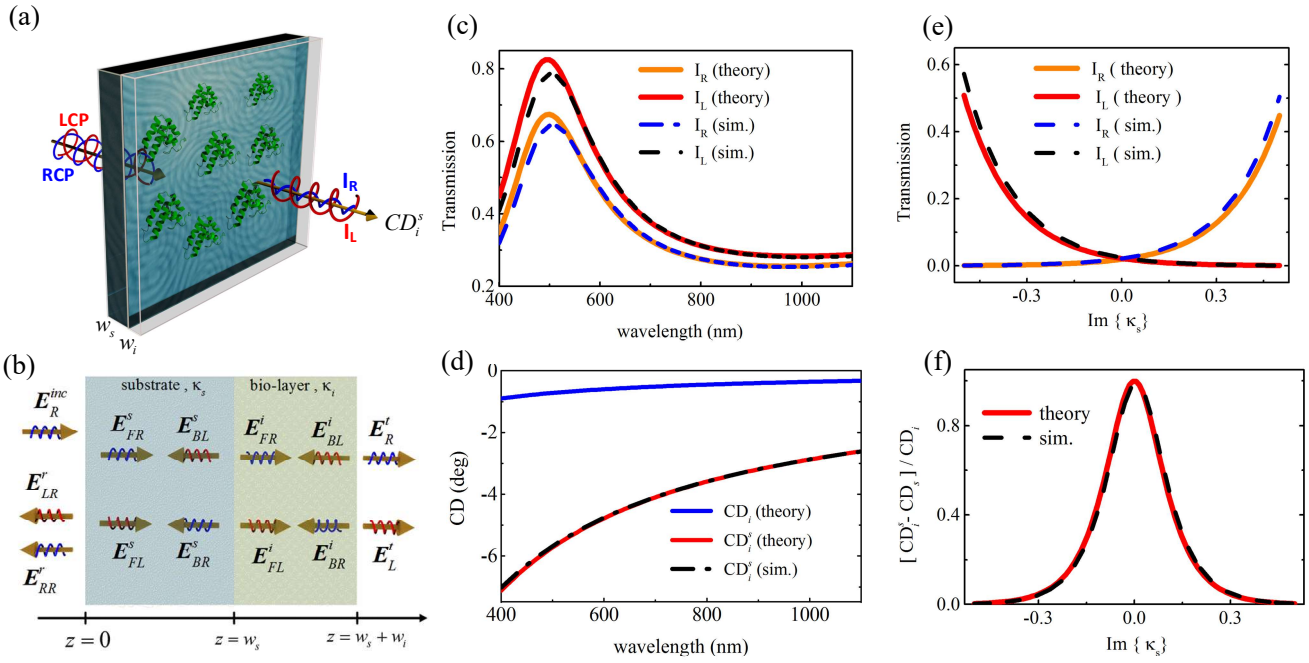

Figure 2. Substrate CD spectroscopy. (a) A chiral bio-layer of thickness w_i placed on top of a simple chiral substrate of thickness w_s, with the whole system being excited by RCP (blue) and LCP (red) light. (b) The configuration in (a), modeled as two homogenous juxtaposed chiral layers of thicknesses and Pasture parameters of, w_i, κ_i (for bio-layer) and w_s, κ_s (for substrate), placed in free space and illuminated under RCP light excitation. With their corresponding nomenclature, the incidence (*inc*), reflected (*r*), internal (*s* for substrate and *i* for bio-layer) and transmitted (*t*) electric field waves are shown schematically. *R* (*L*) stands for right (left) circular polarization and *F* (*B*) stands for forward (backward) propagating light. (c) Transmission intensities and (d) CD_i^s for a bio-layer of thickness 10 *nm* placed on top of a substrate of thickness 70 *nm,* where the refractive indices and Pasture parameters are assumed to be $n_i = 2-.1\mathrm{j},\ \kappa_i = .2-.05\mathrm{j}$ (bio-layer) and $n_s = 3.5-.1\mathrm{j},\ \kappa_s = .5-.05\mathrm{j}$ (substrate). (e) Transmission intensities for bio-layer of thickness $\lambda/10$ and $\kappa_i = .2-.05\mathrm{j}$ placed on top of a substrate of thickness $\lambda/2$, as a function of $\mathrm{Im}\{\kappa_s\}$. (f) Normalized desired CD signal of the chiral biofilm as a function of $\mathrm{Im}\{\kappa_s\}$.

A discussion about realistic solutions to this problem is presented in sec. II, where specifically we show how nanophotonic platforms can remove the background noise (first drawback), as well as compensate for the attenuation factor of the *sech* function (second drawback). Figures 2c, d show, respectively, the transmission spectra and CD_i^s signal for a bio-layer of thickness 10 nm placed on top of a substrate of thickness 70nm. It can be seen that the total CD (black/red) has been enhanced compared to the single bio-layer case

(blue), *but this enhancement originates from* CD_s *and cannot be attributed to the handedness of the bio-layer*. In order to further clarify the effect of chiral loss (due to $4\,k_0\,w_s\,\mathrm{Im}\{\kappa_s\}$ term) from the substrate on the desired CD signal ($CD_i^s - CD_s$), in Figs. 2e,f we have studied the problem as a function of the imaginary part of the substrate Pasture parameter. In Fig. 2e the transmission intensities are obtained for a bio-layer of thickness $\lambda/10$ placed on top of a substrate of thickness $\lambda/2$. The imaginary part of κ_s, changes between -0.5 and +0.5. Figure 2f shows the normalized desired CD signal corresponding to the transmission intensities in Fig. 2e, which is in perfect agreement with the *sech* function, as previously indicated analytically in Eq (5). It can be seen that the simulations and the theoretical results are in excellent agreement. From Fig. 2f and Eq. (5) we can readily infer that substrate Pasture parameter with a non-zero imaginary part (i.e. chiral loss) reduces the desired CD signal.

II. CD signal of a bio-layer placed on top of a nanophotonic chiral substrate

Next, we extend our analysis to nanophotonic (nanostructured) substrates, which have been studied numerically and experimentally in literature.[17-27] In order for our analytical formulas in this section to remain valid for chiral or achiral, plasmonic or dielectric substrates we consider the *most general* case of a plasmonic chiral nanophotonic substrate with a chiral biofilm on top.

One of the main difficulties in the analytical treatment of this chiral system is the intricate interaction of an incident plane wave with the nanophotonic structures. In fact, inside the substrate, due to the complex interplay of local fields produced by the incident wave interacting with the meta-inclusions, we encounter fields that are no longer plane waves (unlike the "simple" chiral substrate case examined in sec. I). Assuming that the spacing between the meta-inclusions is much shorter than the wavelength, this complex interaction can be simplified by attributing effective constitutive parameters to the nanophotonic substrate.[38,39] By using these parameters, the substrate is described as a homogenous matter, which allows for considering plane-wave fields *inside the substrate*. The second challenge in the analytical treatment is associated with the near-field interaction of the chiral substrate with the bio-layer. We know that the effective parameters are associated with the *far-field* reflection and transmission of such structures. On the other hand, nanophotonic structures change, both, the intensity and chirality of the light in their vicinity (near field). We define the local intensity- and local chirality-enhancement factors as $\Im_p^{loc} = |\boldsymbol{E}|^2_{Near} \big/ |\boldsymbol{E}|^2_{Far}$ and $\chi_p^{loc} = \mathrm{Im}\{\boldsymbol{E}.\boldsymbol{H}^*\}_{Near} \big/ \mathrm{Im}\{\boldsymbol{E}.\boldsymbol{H}^*\}_{Far}$, respectively, where the "*Near*" and "*Far*" subscripts refer to the near- and far-field zones, and "*p*" can be either *R* or *L* denoting the polarization of the input excitation. The near-field (far-field) zone is defined as a volume of the same size as the chiral sample, immediately on top of the substrate (at the end of the physical simulation domain). The chiral sample is placed in these two different zones and the local factors are calculated by using the corresponding field values at each point inside the chiral sample (see SI for more details.). By the so-defined enhancement factors, it can be shown (see SI.) that the effective values for the imaginary parts of the permittivity and Pasture parameter of the bio-layer are modified by the factor of $\Im_p$ and χ_p, which are, respectively, the averaged values of $\Im_p^{loc}$ and χ_p^{loc} taken over the chiral sample. It should be noted that, these averaged enhancement factors account for the coupling effects between the nanophotonic substrate and the chiral sample, since the field values (***E*** and ***H***) used in the calculations of these enhancement factors take into account the presence of both the chiral sample and the

substrate. Furthermore, it is to be mentioned that the averaged optical chirality embodies the uniformity of the chiral fields, which is critically important in CD enhancement due to the fact that in realistic implementation of chiral sensing the chiral bio-layer is placed uniformly over the nanophotonic structures and not only on the chiral hotspots.[36]
Now we are able to cope with the second challenge in the analytical treatment of the problem at hand, and model the near-field interaction between the nanophotonic substrate and the chiral sample by embedding intensity- and chirality-enhancement factors in the effective permittivity and the effective Pasture parameter of the sensed bio-layer. By attributing the obtained effective Pasture parameter and permittivity to the bio-layer, and then retrieving the CD signal from Eq. (1), we arrive at the following expression for the total CD_i^m output,

$$CD_i^m = CD_m + \left\{ \frac{k_0 w_i \,\mathrm{Im}\{\varepsilon_i\}}{2\sqrt{\mathrm{Re}\{\varepsilon_i\}}} \left(\Im_L - \Im_R\right) + \frac{CD_i}{2}\left(\chi_R + \chi_L\right) \right\} \mathrm{sech}\left(4 k_0 w_m \,\mathrm{Im}\{\kappa_m\}\right), \qquad (6)$$

where CD_m is the CD contribution of the substrate (without the bio-layer), which can be obtained by inserting its corresponding parameters (κ_m, w_m) in Eq. (3). Equation (6) analytically explains two different effects of substrate chiral absorption $(k_0 w_m \,\mathrm{Im}\{\kappa_m\})$ in nanophotonic CD spectroscopy. The first effect is that it produces an unwanted background noise of CD_m – which has been considered in previous works,[14, 32] but we herein obtained it analytically, in Eq. (3). The second effect, which to our knowledge has not been pointed out before, is the attenuation role of the chiral absorption on the output CD, originating from the evanescent nature of the *sech* function. This is also emphasized in the analysis of section I. Lastly, our closed-form expression in Eq. (6) elucidates analytically that the total output CD depends not only on the chirality of the bio-layer but also on the bio-layer's permittivity. This is a restatement of the fact that if the system is illuminated with two fields of different intensities (i.e. as in the case with two different near-field intensity enhancements) the subtraction of their corresponding difference will be non-zero and depends on the permittivity.

Equation (6) and its associated implications are the key findings of the present work, summarizing the contributing factors for improving the CD signal retrieved from chiral samples using nanophotonic substrates. According to this equation, the optimum nanophotonic-platform candidates for substrate CD spectroscopy are those that feature: *i*) small values of $4\, k_0\, w_m\, \mathrm{Im}\{\kappa_m\}$ to remove CD_m and make the *sech* argument zero; *ii*) equal intensity-enhancement factors for RCP $(\Im_R)$ and LCP $(\Im_L)$ to eliminate the permittivity dependency in Eq. (6); and *iii*) high optical chirality in their near-field zones to maximize the term $\chi_R + \chi_L$. These three requirements help to clarify the tradeoffs in the conception of substrate CD-enhancement platforms. The first class of structures can be provided by thin metasurfaces $(k_0 w_m \to 0)$, lossless dielectrics $(\mathrm{Im}\{\kappa_m\} = 0)$ or achiral $(\kappa_m = 0)$ nanophotonic structures. The second one requires achiral structures, interacting

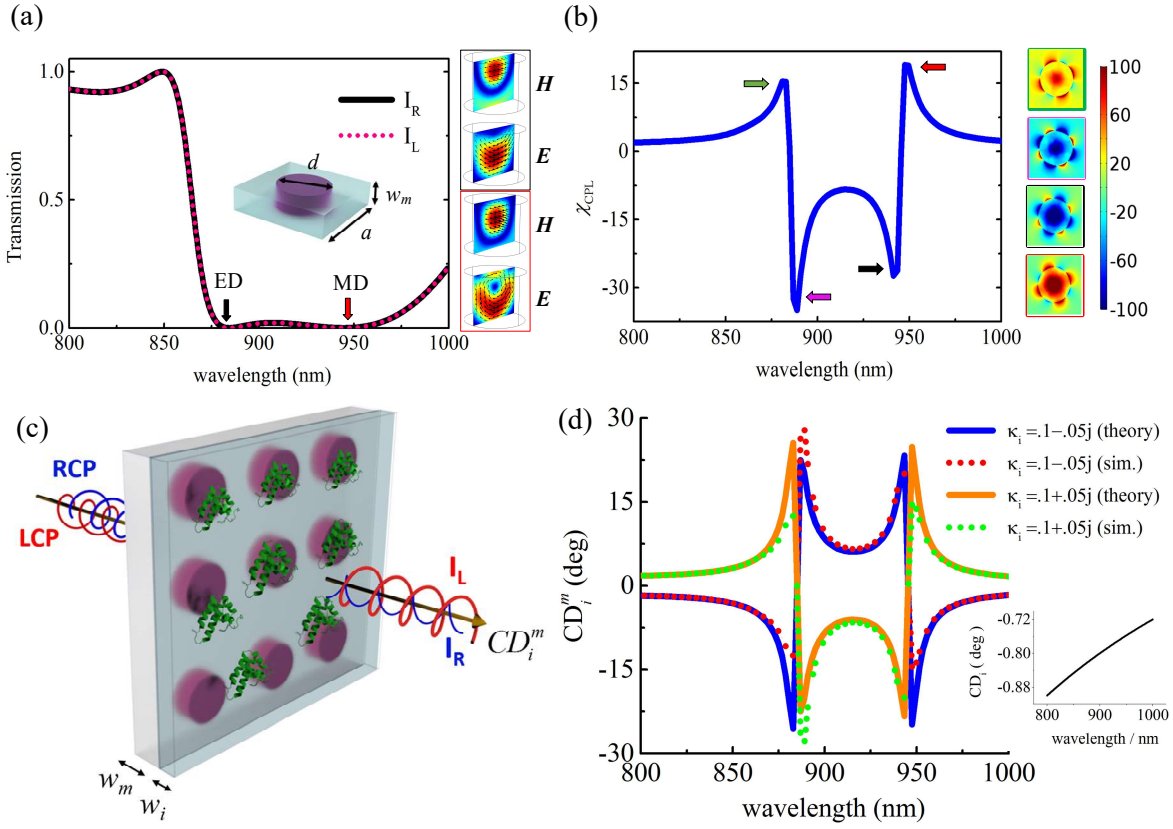

Figure 3. Nanophotonic-substrate CD spectroscopy. (a) Transmission spectra of RCP (I_R) and LCP (I_L) waves for the proposed achiral dielectric substrate. The structure is composed of silicon nanodisks of diameter d=290 nm and height w_m = 220 nm, with a lattice constant of a=490 nm, and embedded into a homogenous dielectric of refractive index of n=1.5. The inset shows a unit cell of the structure. The transmission spectra show two resonance dips at 885 nm and 945 nm, which arise from an electric dipole (ED) and a magnetic dipole (MD) response, respectively, of the silicon nanodisks. The mode profiles at ED and MD resonances are shown by black and red square panels, respectively. (b) Averaged optical chirality enhancement factor for the proposed nanophotonic substrate. The color panels show the local optical chirality enhancement at the ED and MD resonances in the near-field zone of the structure. (c) The chiral sample with refractive index of $n_i = 1.45 - .1\mathrm{j}$ and Pasture parameter of $\kappa_i = .1 \pm .05\mathrm{j}$, placed on top of the proposed substrate. The whole system is excited by RCP (blue) and LCP (red) light, and the CD_i^m at the output side measures the total differential absorbance of the system. (d) Calculated CD_i^m signal, as obtained by analytic theory and simulations, for two chiral samples with different signs of Pasture parameter. Inset shows the chirality of the bio-film alone.

with either RCP or LCP waves in the same manner, thereby leading to $\Im_R = \Im_L$ in the near-field zone of the structure. The third class can be afforded by, both, chiral or achiral structures, but generally the chiral ones have higher amounts of optical chirality compared to their achiral counterparts.[14]

Based on all of the aforementioned considerations, herein we introduce an achiral dielectric nanophotonic substrate, composed of silicon nanodisks (of refractive index $n_d = 3.5$), embedded in a homogenous dielectric with refractive index of $n = 1.5$. This proposed platform allows for all of above-mentioned features, and has a simplified CD signal of

$$CD_i^m = \chi_{CPL}\, CD_i, \quad (7)$$

where χ_{CPL} is the chirality-enhancement factor for either RCP or LCP waves. It is evident from Eq. (7) that this structure features a background-free CD signal, which is only dependent on the handedness of the bio-layer, amplified by a factor of χ_{CPL}.

Figure 3(a) presents the transmission spectra for RCP and LCP waves, with the disk diameter (d) and height (w_m) being 220 nm and 290 nm respectively (inset). We note that the two transmissions are identical, implying a vanishing CD_m background signal. On the other hand, the transmission spectra shows two resonance dips at $\lambda = 885nm$ and $\lambda = 945nm$, which arise from an electric dipole (ED) and magnetic dipole (MD) response of the silicon nanodisks, respectively (cf. field patterns in Fig. 3(a)). Figure 3(b) shows the chirality-enhancement factor for the proposed platform. It is evident that the ED and MD resonances are well capable of providing high optical chirality at their corresponding wavelengths, as well as providing considerable optical chirality between the two resonances. These chiral near-fields appear in dielectric structures with high refractive index at multipolar Mie resonances.[40] Thus, this dielectric achiral substrate still offers high optical chirality – which generally characterizes plasmonic chiral structures. It is important to note that at the two sides of both resonances the sign of the optical chirality is reversed, implying a corresponding change to the sign of the CD signal when a bio-layer is placed on top of the substrate.

Figure 3(c) illustrates a chiral sensing configuration by our proposed platform, in which a chiral sample of thickness 20 nm and Pasture parameter $\kappa_m = .1 - .05\mathrm{j}$ is placed on top of the introduced nanophotonic substrate, and the whole system is excited by RCP (blue) and LCP (red) light. The CD_i^m at the output side measures the total differential absorbance of the system for RCP and LCP illuminations, which for this special platform arises only from the bio-layer chirality ($\mathrm{Im}\{\kappa_i\}$). In Fig. 3(d) we have calculated the CD_i^m signal theoretically (solid blue) and by full-wave simulations (dotted red). It can be seen that the theoretical and the simulation results are in excellent agreement. The inset in Fig. 3(d) shows the CD signal of the bio-layer without substrate, which is only about 0.80 degree. It should be noted that, in addition to removing the background noise and permittivity dependency, this platform provides extremely high CD enhancement, of the order of 30 at the resonances and ~10-20 between the resonances. In order to check that the CD signal is only dependent on the handedness of the sample, we have studied another bio-layer of Pasture parameter $\kappa_m = .1 + .05\mathrm{j}$. We assumed that the two bio-layers are only different in their CD signatures, not in their ORD responses, which corresponds to different signs for the imaginary part of the Pasture parameter. If the platform does not have any background noise and is not permittivity-dependent, then by changing the handedness of the bio-layer the CD signal should be digitally reversed in sign. Figure 3(d) shows the theoretical (solid orange) and simulation (dotted green) results for this second bio-layer. It is seen that the simulation and theoretical results are again in an excellent agreement, and the CD signal is digitally reversed with respect to the first bio-layer, as expected.

In conclusion, the above discussions and results reveal that the herein-developed analytical closed-form expressions of substrate-enhanced chiral sensing accurately characterize the response of these structures, and help to guide their optimal design. Our analysis is inherently capable of treating all kinds of nanophotonic chiral-sensing platforms, including plasmonic or dielectric, chiral or achiral, three-dimensional or thin surface structures (metasurfaces), and on this basis we identified an optimal, dielectric, achiral class of such structures for enhanced, background-free chiral sensing. Our results

corroborate and extend previously reported aspects of such structures, highlighting overlooked features of substrate-enhanced chiral light-matter interactions, and providing overall an analytic insight at the tradeoffs that are to be accommodated in the optimal design of these intricate configurations.

AUTHOR INFORMATION

Corresponding Author

*Email: hatice.altug@epfl.ch

ACKNOWLEDGMENTS

We acknowledge the support of the European Commission Horizon 2020 (grant no. FETOPEN-737071) ULTRA-CHIRAL Project, and "EPFL Fellows" Co-found Marie-Curie Fellowship for K.L.T. Also funding from Ministry of Science, Research and Technology of Islamic Republic of Iran is gratefully acknowledged.

REFERENCES

[1] Barron, Laurence D. "Chirality and life." Space Science Reviews 135, no. 1-4 (2008): 187-201.

[2] Dobson, Christopher M. "Protein folding and misfolding." Nature 426, no. 6968 (2003): 884-890

[3] Davies, Neal M., and Xiao Wei Teng. "Importance of chirality in drug therapy and pharmacy practice: Implications for psychiatry." Advances in Pharmacy 1, no. 3 (2003): 242-252.

[4] Smith, Silas W. "Chiral toxicology: it's the same thing… only different." Toxicological sciences 110, no. 1 (2009): 4-30.

[5] Boriskina, Svetlana, and Nikolay I. Zheludev, eds. Singular and Chiral Nanoplasmonics. CRC Press, 2014.

[6] Barron, Laurence D. Molecular light scattering and optical activity. Cambridge University Press, 2004.

[7] Nordén, Bengt. Circular dichroism and linear dichroism. Vol. 1. Oxford University Press, USA, 1997.

[8] Lindell IV, Sihvola AH, Tretyakov SA, Viitanen AJ. Electromagnetic waves in chiral and bi-isotropic media.

[9] Tsakmakidis KL, Boyd RW, Yablonovitch E, Zhang X. Large spontaneous-emission enhancements in metallic nanostructures: towards LEDs faster than lasers. Optics express. 2016 Aug 8;24(16):17916-27.

[10] Tsakmakidis KL, Hess O, Boyd RW, Zhang X. Ultraslow waves on the nanoscale. Science. 2017 Oct 20;358(6361):eaan5196.

[11] Valev VK, Baumberg JJ, Sibilia C, Verbiest T. Chirality and chiroptical effects in plasmonic nanostructures: fundamentals, recent progress, and outlook. Advanced Materials. 2013 May 14;25(18):2517-34.

[12] Hendry E, Mikhaylovskiy RV, Barron LD, Kadodwala M, Davis TJ. Chiral electromagnetic fields generated by arrays of nanoslits. Nano letters. 2012 Jun 11;12(7):3640-4.

[13] Luo, Yang, Cheng Chi, Meiling Jiang, Ruipeng Li, Shuai Zu, Yu Li, and Zheyu Fang. "Plasmonic Chiral Nanostructures: Chiroptical Effects and Applications." Advanced Optical Materials (2017).

[14] Schäferling, Martin. Chiral Nanophotonics: Chiral Optical Properties of Plasmonic Systems. Vol. 205. Springer, 2016.

[15] Gansel, Justyna K., Michael Thiel, Michael S. Rill, Manuel Decker, Klaus Bade, Volker Saile, Georg von Freymann, Stefan Linden, and Martin Wegener. "Gold helix photonic metamaterial as broadband circular polarizer." Science 325, no. 5947 (2009): 1513-1515.

[16] Esposito, Marco, Vittorianna Tasco, Massimo Cuscunà, Francesco Todisco, Alessio Benedetti, Iolena Tarantini, Milena De Giorgi, Daniele Sanvitto, and Adriana Passaseo. "Nanoscale 3D chiral plasmonic helices with circular dichroism at visible frequencies." ACS Photonics 2, no. 1 (2014): 105-114.

[17] Frank, Bettina, Xinghui Yin, Martin Schäferling, Jun Zhao, Sven M. Hein, Paul V. Braun, and Harald Giessen. "Large-area 3D chiral plasmonic structures." ACS nano 7, no. 7 (2013): 6321-6329.

[18] Decker, M., M. Ruther, C. E. Kriegler, J. Zhou, C. M. Soukoulis, S. Linden, and M. Wegener. "Strong optical activity from twisted-cross photonic metamaterials." Optics letters 34, no. 16 (2009): 2501-2503.

[19] Zhao, Y., M. A. Belkin, and A. Alù. "Twisted optical metamaterials for planarized ultrathin broadband circular polarizers." Nature communications 3 (2012): 870.

[20] Hentschel, Mario, Martin Schäferling, Thomas Weiss, Na Liu, and Harald Giessen. "Three-dimensional chiral plasmonic oligomers." Nano letters 12, no. 5 (2012): 2542-2547.

[21] Guerrero-Martínez, Andrés, Baptiste Auguié, José Lorenzo Alonso-Gómez, Zoran Džolić, Sergio Gómez-Graña, Mladen Žinić, M. Magdalena Cid, and Luis M. Liz-Marzán. "Intense Optical Activity from Three-Dimensional Chiral Ordering of Plasmonic Nanoantennas." Angewandte Chemie International Edition 50, no. 24 (2011): 5499-5503.

[22] Fan, Zhiyuan, and Alexander O. Govorov. "Plasmonic circular dichroism of chiral metal nanoparticle assemblies." Nano letters10, no. 7 (2010): 2580-2587.

[23] Hendry, Euan, T. Carpy, J. Johnston, M. Popland, R. V. Mikhaylovskiy, A. J. Lapthorn, S. M. Kelly, L. D. Barron, N. Gadegaard, and M. Kadodwala. "Ultrasensitive detection and characterization of biomolecules using superchiral fields." Nature nanotechnology 5, no. 11 (2010): 783-787.

[24] Kwon, Do-Hoon, Pingjuan L. Werner, and Douglas H. Werner. "Optical planar chiral metamaterial designs for strong circular dichroism and polarization rotation." Optics express 16, no. 16 (2008): 11802-11807.

[25] Kaschke, Johannes, and Martin Wegener. "Gold triple-helix mid-infrared metamaterial by STED-inspired laser lithography." Optics letters 40, no. 17 (2015): 3986-3989.

[26] Yoo, SeokJae, Minhaeng Cho, and Q-Han Park. "Globally enhanced chiral field generation by negative-index metamaterials." Physical Review B 89, no. 16 (2014): 161405.

[27] Davis, T. J., and E. Hendry. "Superchiral electromagnetic fields created by surface plasmons in nonchiral metallic nanostructures." Physical Review B 87, no. 8 (2013): 085405.

[28] García-Etxarri, Aitzol, and Jennifer A. Dionne. "Surface-enhanced circular dichroism spectroscopy mediated by nonchiral nanoantennas." Physical Review B 87, no. 23 (2013): 235409.

[29] Tang, Yiqiao, and Adam E. Cohen. "Enhanced enantioselectivity in excitation of chiral molecules by superchiral light." Science 332, no. 6027 (2011): 333-336.

[30] Tang, Yiqiao, and Adam E. Cohen. "Optical chirality and its interaction with matter." Physical review letters 104, no. 16 (2010): 163901.

[31] Schäferling, Martin, Daniel Dregely, Mario Hentschel, and Harald Giessen. "Tailoring enhanced optical chirality: design principles for chiral plasmonic nanostructures." Physical Review X 2, no. 3 (2012): 031010.

[32] Zhao, Yang, Amir N. Askarpour, Liuyang Sun, Jinwei Shi, Xiaoqin Li, and Andrea Alù. "Chirality detection of enantiomers using twisted optical metamaterials." Nature communications 8 (2017).

[33] Yin X, Schäferling M, Metzger B, Giessen H. Interpreting chiral nanophotonic spectra: the plasmonic Born–Kuhn model. Nano letters. 2013 Nov 27;13(12):6238-43.

[34] Govorov AO, Fan Z, Hernandez P, Slocik JM, Naik RR. Theory of circular dichroism of nanomaterials comprising chiral molecules and nanocrystals: plasmon enhancement, dipole interactions, and dielectric effects. Nano letters. 2010 Feb 25;10(4):1374-82.

[35] Schäferling M, Engheta N, Giessen H, Weiss T. Reducing the complexity: Enantioselective chiral near-fields by diagonal slit and mirror configuration. ACS Photonics. 2016 May 20;3(6):1076-84.

[36] Nesterov ML, Yin X, Schäferling M, Giessen H, Weiss T. The role of plasmon-generated near fields for enhanced circular dichroism spectroscopy. ACS Photonics. 2016 Apr 1;3(4):578-83.

[37] Poulikakos LV, Gutsche P, McPeak KM, Burger S, Niegemann J, Hafner C, Norris DJ. Optical chirality flux as a useful far-field probe of chiral near fields. ACS Photonics. 2016 Aug 9;3(9):1619-25.

[38] Zhao, Rongkuo, Thomas Koschny, and Costas M. Soukoulis. "Chiral metamaterials: retrieval of the effective parameters with and without substrate." Optics express 18, no. 14 (2010): 14553-14567.

[39] Chen, Xudong, Tomasz M. Grzegorczyk, Bae-Ian Wu, Joe Pacheco Jr, and Jin Au Kong. "Robust method to retrieve the constitutive effective parameters of metamaterials." Physical Review E 70, no. 1 (2004): 016608.

[40] Ho CS, Garcia-Etxarri A, Zhao Y, Dionne J. Enhancing enantioselective absorption using dielectric nanospheres. ACS Photonics. 2017 Jan 26;4(2):197-203.

For Table of Contents Use Only